

# Phenol degradation by advanced electrochemical oxidation process electro-Fenton using a carbon felt cathode

Marcio Pimentel<sup>a,b</sup>, Nihal Oturan<sup>a</sup>, Marcia Dezotti<sup>b</sup>, Mehmet A. Oturan<sup>a,\*</sup>

<sup>a</sup> *Université Paris-Est, Laboratoire Géomatériaux et Géologie de l'Ingénieur, 5 Boulevard Descartes,  
Champs-sur-Marne, Bâtiment IFI, 77454 Marne-la-Vallée Cedex 2, France*

<sup>b</sup> *Chemical Engineering Program - COPPE, Federal University of Rio de Janeiro, P.O. Box 68502, 21941-972 Rio de Janeiro, Brazil*

Received 14 November 2007; received in revised form 24 January 2008; accepted 4 February 2008

Available online 20 February 2008

## Abstract

Oxidation of phenol in aqueous media by electro-Fenton process using carbon felt cathode has been studied. The salts of iron, cobalt, manganese, and copper were used to provide the metal cations as catalyst of Fenton reaction to produce hydroxyl radicals.  $10^{-4}$  M of soluble iron(II) sulfate salt supplied the optimum catalytic condition, allowing to remove 100% of total organic carbon (TOC) of aqueous phenol solutions. The main reaction intermediates formed during electro-Fenton treatment were identified as hydroquinone, *p*-benzoquinone, and catechol. Carboxylic acids such as maleic, fumaric, succinic, glyoxylic, oxalic, and formic were predominantly identified as end products, before complete mineralization. The absolute rate constant of phenol degradation by hydroxyl radicals was obtained in acid medium ( $2.5 < \text{pH} < 3.0$ ), being equal to  $(2.62 \pm 0.23) \times 10^9 \text{ M}^{-1} \text{ s}^{-1}$ . Experiments with electro-Fenton oxidation of each aromatic intermediate allowed to propose a complete mineralization pathway.

© 2008 Elsevier B.V. All rights reserved.

**Keywords:** Advanced oxidation process; Electro-Fenton; Phenol; Mineralization; Catalysts

## 1. Introduction

Among the various wastes, phenolic compounds constitute a family of pollutants particularly toxic to the aquatic fauna and flora. These compounds are released in the surface water by a considerable number of industries, mainly, by pharmaceutical plants, oil refineries, coke plants, pulp, and food-processing industries and several other chemical plants [1,2], constituting an environmental hazard. Phenol is also a typical molecule present in most of aromatic products, emphasizing its relevance. It is toxic to fish at a 1–2-ppm concentration level [3], being considered lethal to most of aquatic organisms exposed to concentrations of 10–100 ppm [4]. Moreover, it presents an acute toxicity for man [5]. Consequently, phenol removal from wastewater is an environmental concern.

Phenol belongs to the recalcitrant pollutants to conventional physicochemical and biological treatments. On the other hand, the advanced oxidation processes (AOPs) have been defined as

effective processes for treatment of wastewater containing toxic and persistent organic pollutants. These processes use hydroxyl radical, a powerful oxidizing agent, which is able to destruct target pollutants [6]. The oxidative degradation of phenol in aqueous media has been the subject of several AOPs studies such as Fenton's reagent [7], Fenton like process using zero valence iron [8], ozonation [9],  $\text{H}_2\text{O}_2$ -mediated photodegradation [10], photo-Fenton [10,11], and heterogeneous photocatalysis [12,13]. However, high cost of chemical products, parasite reactions, strict applying conditions and/or moderate mineralization efficiency limit most of the AOPs. Esplugas et al. [14], for instance, studied the mineralization of synthetic samples of phenol (1 mM) by different advanced oxidation processes. In best conditions, low total organic carbon (TOC) decreases of 10, 37, 45, and 65% were obtained for Fenton,  $\text{O}_3/\text{H}_2\text{O}_2$ ,  $\text{O}_3/\text{H}_2\text{O}_2/\text{UV}$ , and  $\text{O}_3/\text{UV}$  systems, respectively. The chemical oxygen demand (COD) abatement was 30% in optimum conditions in the study of Pouloupoulos et al. [15] during the degradation of 3.2 mM phenol aqueous solution by  $\text{H}_2\text{O}_2/\text{UV}$  system.

Electrochemistry offers new ways for organic waste treatment. The advanced electrochemical oxidation processes (AEOPs) such as anodic oxidation [16–18], electro-Fenton

\* Corresponding author. Tel.: +33 149 32 90 65; fax: +33 149 32 91 37.

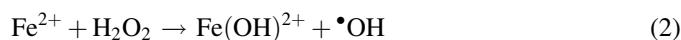
E-mail address: [oturan@univ-mlv.fr](mailto:oturan@univ-mlv.fr) (M.A. Oturan).

[19–22], electro-Fenton coupled to anodic oxidation [23–25], solar photo-electro-Fenton [26], and other electro-Fenton like processes [27,28] developed during the last decade constitute emergent and promising AOPs. Moreover numerous works have been conducted by anodic oxidation to degrade phenol in aqueous solution using various anodes such as Pt [29], PbO<sub>2</sub> [16], bismuth-doped PbO<sub>2</sub> [30], Ti/SnO<sub>2</sub>–Sb [31], and boron-doped diamond [32,33]. Fockedeey and Van Lierde [34] studied the electrochemical oxidation of phenol by the coupling of anodic and cathodic reactions, provided by Sb-doped-SnO<sub>2</sub>-coated titanium anode and a reticulated vitreous carbon cathode.

In this work, we have studied the oxidative degradation of aqueous phenols solutions in acidic medium by electro-Fenton process using a carbon felt cathode and a platinum anode in order to evaluate the mineralization efficiency of this process. The process is based on the electrochemical in situ production of the Fenton's reagent, a mixture of ferrous ions (used as catalyst) and hydrogen peroxide which is able to generate hydroxyl radicals [35,36]. Hydrogen peroxide is continuously generated in acidic-contaminated medium from the two-electron reduction of dissolved O<sub>2</sub>. New catalysts have been used in other electrochemical experiments with carbon felt cathode to assure Fenton like reactions. These studies evidenced that pH 3 enhances hydrogen peroxide electrochemical production [27,37]. In fact, considering saturated concentration of oxygen in experimental conditions (0.45 mM < [O<sub>2</sub>] < 0.58 mM), pH 3 assures ideal conditions ([H<sup>+</sup>]/[O<sub>2</sub>] ≅ 2) to optimize electrochemical production of hydrogen peroxide according to the following equation, avoiding the formation of peroxo and sulfate complexes in higher acid mediums [38]:



Addition of a catalytic amount of ferric or ferrous ions in the solution to be treated allows an enhancement of the oxidation power of electrogenerated H<sub>2</sub>O<sub>2</sub> according to the Fenton's reaction (reaction (2)):



At pH 3 (optimal value for reaction (1)), the predominant species of Fe(III) is Fe(OH)<sup>2+</sup> and the electrochemical reduction is written according to reaction (3):



The sum of reactions (2) + (3) indicates the electrocatalysis of the Fenton's reaction.

On the other hand, the production of H<sub>2</sub>O<sub>2</sub> is also electrocatalyzed because the oxygen required by reaction (1), can be produced by water oxidation at the Pt anode (reaction (4)):



Hydroxyl radicals are produced in a catalytic and controlled way, allowing the mineralization of organic pollutants (transformation to CO<sub>2</sub>, H<sub>2</sub>O and/or mineral ions) [16–28].

The classical electro-Fenton process is carried out with one of the forms of the Fe<sup>3+</sup>/Fe<sup>2+</sup> redox couple ( $E^0 = 0.77$  V/NHE). However, any appropriate homogeneous redox couple M<sup>(n+1)+</sup>/M<sup>n+</sup> can be used according to reaction (5):



Several metal cations have been tested as catalysts [39,40]. In this case, electro-Fenton process efficiency is influenced by the standard potential of M<sup>(n+1)+</sup>/M<sup>n+</sup> redox couple used and by scavenging catalyst effect.

This paper reports an investigation concerning the effect of catalyst nature and concentration on the electro-Fenton degradation of phenol and the mineralization efficiency of this technique to treat phenol aqueous solutions. We have carried out a detailed study in aqueous medium to show the viability of the electro-Fenton process to remove phenol and its hydroxylated and/or quinoid metabolites from wastewater. The effect of the nature of catalyst was studied by comparative treatments with several metal cations such as Fe<sup>2+</sup> ( $E^0_{(\text{Fe}^{3+}/\text{Fe}^{2+})} = 0.77$  V), Co<sup>2+</sup> ( $E^0_{(\text{Co}^{3+}/\text{Co}^{2+})} = 1.92$  V), Cu<sup>2+</sup> ( $E^0_{(\text{Cu}^{2+}/\text{Cu}^+)} = 0.16$  V), and Mn<sup>2+</sup> ( $E^0_{(\text{Mn}^{3+}/\text{Mn}^{2+})} = 1.50$  V). The aromatic and aliphatic intermediates formed during current-controlled electrolyses were identified by chromatographic techniques. The follow of the phenol decay and evolution of its oxidation reaction intermediates during electro-Fenton treatment as well as the TOC removal measurements permitted to propose a plausible mineralization pathway of phenol, including hydroxyl radical reactions which controlled the destruction of phenol and predominant aromatics. Competitive kinetics method [37,41] using equal initial concentrations of phenol and 4-hydroxybenzoic acid (4-HBA) allowed to obtain the absolute rate constant of phenol degradation by hydroxyl radicals in pH 3. The effect of current density and initial volume on mineralization rates was also studied.

## 2. Experimental

### 2.1. Chemicals

Phenol (Aldrich, 99.5%) was used as soon as purchased. The salts used to obtain catalyst ions (iron(II) sulfate heptahydrate, 99.75%, copper(II) sulfate pentahydrate, 98%, cobalt(II) sulfate heptahydrate, 99%, and manganese(II) sulfate monohydrate, 98%) were supplied by Acros Organics and Fluka and were used without further purification. Catalyst concentrations used in different experiments are outlined in Table 1. All other products used, including intermediates, were obtained with purity higher than 99%.

All solutions were prepared with pure water obtained from a Millipore Simplicity 185 system (conductivity < 6 × 10<sup>−8</sup> S cm<sup>−1</sup> at 25 °C). The pH of solutions was adjusted using analytical grade sulfuric acid (Merck).

Table 1  
Metal ions and salt concentrations used during catalyst's experiments

Metal ions (catalyst)	Salt	Concentrations (mM)
$\text{Co}^{2+}$	$\text{CoSO}_4 \cdot 5\text{H}_2\text{O}$	0.05
		0.10
		1.00
$\text{Cu}^{2+}$	$\text{CuSO}_4 \cdot 5\text{H}_2\text{O}$	1.00
		5.00
		10.00
$\text{Fe}^{2+}$	$\text{FeSO}_4 \cdot 7\text{H}_2\text{O}$	0.05
		0.10
		1.00
$\text{Mn}^{2+}$	$\text{MnSO}_4 \cdot \text{H}_2\text{O}$	0.10
		0.50
		1.00

## 2.2. Electrochemical cell

Experiments were performed at room temperature ( $25 \pm 1^\circ\text{C}$ ) in a 0.40-L open and undivided cylindrical glass cell of internal diameter equal to 60 mm, equipped with two electrodes totally immersed in the solutions under study. The cathode was a piece of carbon felt ( $6\text{ cm} \times 8\text{ cm} \times 0.6\text{ cm}$ ) which was placed on the inner wall of the cell. The anode was a cylindrical Pt grid placed in the centre of the cell. Solutions were continuously stirred with a magnetic bar (500 rotations per min). During experiments to study the effect of current density, it was also used a larger piece of carbon felt ( $6\text{ cm} \times 17\text{ cm} \times 0.6\text{ cm}$ ). A control experiment was conducted using a larger cathode surface and a smallest initial volume in order to quantify phenol adsorption on carbon felt electrode.

Experiments were monitored by an EG&G Princeton Applied Research 273A potentiostat/galvanostat. Prior to the electrolysis, compressed air was bubbled for 10 min through the solution. A catalytic quantity of metal ion (catalyst) was added to solutions before starting the electrolysis. Current remained constant during electrolysis and samples were withdrawn at regular coulometric charges. The initial pH of solutions was adjusted to three by sulfuric acid and remained almost constant. This pH was chosen in order to optimize the production of hydroxyl (Eqs. (1) and (5)) and to avoid the formation of peroxo and sulfate complex. The pH was measured by a pH glass electrode calibrated with standard buffers at pH values of 4 and 7. The ionic strength was maintained constant by addition of 50 mM of  $\text{Na}_2\text{SO}_4$  to improve the conductivity of the medium, especially with higher currents.

Optimum catalyst conditions were obtained in two steps. Firstly, electrolyses were conducted at constant current and phenol initial concentration during 4 h. Catalysts of different nature and concentrations were tested and runs were monitored by TOC analyses. Results were compared and allowed to obtain the best one. Then, kinetic experiments of phenol aqueous solutions were carried out to identify the best concentration for the optimized catalyst.

Additional experiments were conducted in optimum catalyst and concentration conditions and several phenol oxidation intermediates were identified. The electro-Fenton degradation of each aromatic intermediate permitted to propose a complete mechanism to phenol mineralization.

## 2.3. Analysis procedures

Phenol and all other aromatics were identified and quantified by reverse phase chromatography using a Lachrom-Merck HPLC chromatograph controlled by a EZCHROM elite program. It was fitted with a quaternary pump MH L-7100, a Merck column oven L-7360 with thermostat at  $40^\circ\text{C}$  and a Purospher RP-C18 column ( $5\text{ }\mu\text{m}$ ,  $250\text{ mm} \times 4.6\text{ mm}$ ) coupled with a photodiode array detector (L-7455) at 280 nm. A mixture of water/methanol/acetic acid (79.2/19.8/1, v/v) was used as mobile phase at a flow rate of  $0.8\text{ mL min}^{-1}$ . Carboxylic acids were identified and measured by ion-exclusion chromatography fitted with a Supelcogel H ( $250\text{ mm} \times 4.6\text{ mm}$ ) column at  $40^\circ\text{C}$ . The detection was performed at 210 nm with a mobile phase of 4 mM  $\text{H}_2\text{SO}_4$  at a flow rate of  $0.2\text{ mL min}^{-1}$ . All analyses were made by injecting 20- $\mu\text{L}$  aliquots into the chromatograph. The progress of the mineralization of phenol aqueous solutions during the treatment was monitored by measuring their TOC abatement with a Shimadzu  $\text{V}_{\text{CSH}}$  TOC analyser. Reproducible TOC values were obtained from analysis of 50- $\mu\text{L}$  aliquots, using the standard non-purgeable organic carbon method. During all experiments, samples were collected and immediately measured without using any filter.

Competitive kinetics method [37,41] using 4-HBA as reference compound was employed in order to obtain the absolute rate constant of phenol degradation by hydroxyl radicals.

Three final experiments applying the same current and phenol initial concentration were made to study the effect of volume and current density on mineralization rates.

## 3. Results and discussion

### 3.1. Determination of optimum catalyst conditions

Electrochemical treatments were performed by electrolyzing 0.33 mM aqueous phenol solutions (equivalent to  $24\text{ mg L}^{-1}$  of TOC) in acid medium (pH 3) at constant current of 100 mA for 4 h in order to study the effect of the nature of catalyst on the mineralization efficiency. The comparative TOC abatement of these trials was depicted in Fig. 1.

Different behaviors were observed for iron and cobalt in comparison with copper and manganese. Higher mineralization yields (about 80 and 78% for iron and cobalt, respectively in 4 h of electrolysis) were obtained when 0.1 mM of iron(II) or cobalt(II) ions was employed as catalyst. Stronger changes in color were also observed, which can be explained by the formation of quinones [7,11]. In these cases, catalyst concentrations greater than 0.1 mM harmed the efficiency of the treatment, which can be explained by scavenging reactions

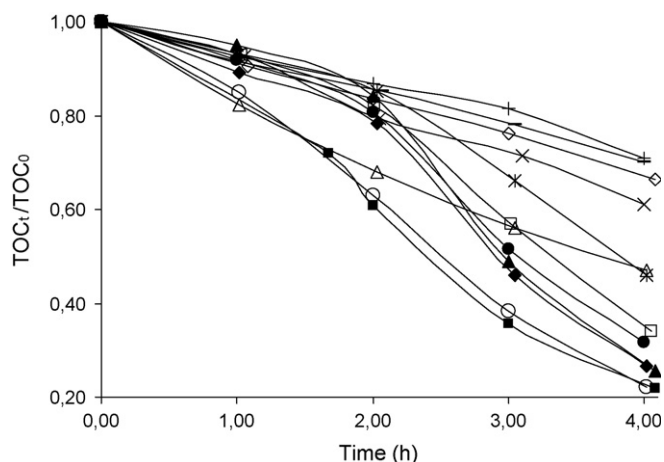
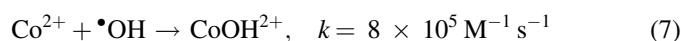
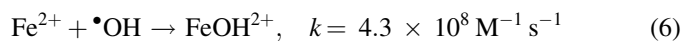
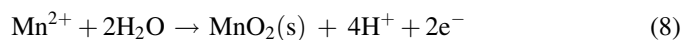


Fig. 1. TOC removal with electrolysis time for the mineralization of 0.33 mM ( $\text{TOC}_0 = 24 \text{ mg L}^{-1}$ ) phenol aqueous solution with different catalysts during electro-Fenton treatment— $[\text{Fe}^{2+}]$ : 0.05 mM ( $\square$ ), 0.10 mM ( $\blacksquare$ ), and 1.00 mM ( $\triangle$ );  $[\text{Co}^{2+}]$ : 0.05 mM ( $\blacktriangle$ ), 0.10 mM ( $\circ$ ), and 1.00 mM ( $\blacklozenge$ );  $[\text{Mn}^{2+}]$ : 0.10 mM ( $-$ ), 0.50 mM ( $\diamond$ ), and 1.0 mM ( $*$ );  $[\text{Cu}^{2+}]$ : 1.0 mM ( $+$ ), 5 mM ( $\bullet$ ), and 10 mM ( $\times$ ). Experimental conditions: initial volume ( $V_0$ ) = 330 mL,  $I$  = 100 mA, and pH 3.

between iron(II) or cobalt(II) ions and hydroxyl radicals [42,43].



When copper or manganese is used as catalyst, optimum catalyst concentration is higher. With low concentration of catalyst, the mineralization yield remains poor in comparison to iron or cobalt (about 35% for 1 mM  $\text{Cu}^{2+}$  or 0.1 mM  $\text{Mn}^{2+}$ ). Optimum mineralization efficiencies were obtained for 5 mM  $\text{Cu}^{2+}$  and 1 mM  $\text{Mn}^{2+}$ , but mineralization rates remained always lower in comparison to iron and cobalt ions as catalyst. During experiments with copper and manganese, metal deposits were observed evidencing changes in catalyst concentrations, decreasing hydroxyl radicals production according to the reaction (5). Cathodic deposition of copper can be justified by the values of the standard reduction potential of Cu(II) ( $E_{\text{Cu}^{2+}/\text{Cu(s)}}^0 = 0.34 \text{ V/SHE}$ ) and Cu(I) ( $E_{\text{Cu}^+/\text{Cu(s)}}^0 = 0.52 \text{ V/SHE}$ ) ions, which favour their easy reduction. During our experiments, cathode potential ( $\cong -0.25 \text{ V/SHE}$ ) [19,35] does not favour deposition of iron ( $E_{\text{Fe}^{2+}/\text{Fe(s)}}^0 = -0.44 \text{ V}$ ,  $E_{\text{Fe}^{3+}/\text{Fe(s)}}^0 = -0.04 \text{ V}$ ) or cobalt ( $E_{\text{Co}^{2+}/\text{Co(s)}}^0 = -0.28 \text{ V}$ ) [44]. Low-manganese efficiency can be explained by the anodic deposition observed during experiments which is reported by several electrochemical studies [45,46] in acidic solutions according to reaction (8):



Considering the toxicity of cobalt for the environment [47], these results highlighted that a concentration about 0.1 mM of ferrous ions constitute the optimal catalyst condition for the degradation of phenol aqueous solutions by electro-Fenton process.

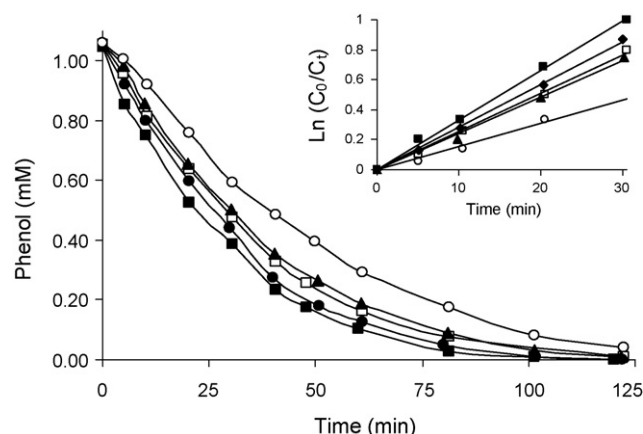


Fig. 2. Effect of catalyst ( $\text{Fe}^{2+}$ ) concentration on the degradation kinetics of phenol at pH 3 during current-controlled electrolysis at 60 mA—( $\square$ )  $[\text{Fe}^{2+}] = 0.05 \text{ mM}$  ( $k_{\text{app}} = 0.028 \text{ min}^{-1}$ ,  $R^2 = 0.997$ ); ( $\blacksquare$ )  $[\text{Fe}^{2+}] = 0.1 \text{ mM}$  ( $k_{\text{app}} = 0.037 \text{ min}^{-1}$ ,  $R^2 = 0.998$ ); ( $\bullet$ )  $[\text{Fe}^{2+}] = 0.25 \text{ mM}$  ( $k_{\text{app}} = 0.034 \text{ min}^{-1}$ ,  $R^2 = 0.999$ ); ( $\blacktriangle$ )  $[\text{Fe}^{2+}] = 0.5 \text{ mM}$  ( $k_{\text{app}} = 0.027 \text{ min}^{-1}$ ,  $R^2 = 0.998$ ); ( $\circ$ )  $[\text{Fe}^{2+}] = 1.0 \text{ mM}$  ( $k_{\text{app}} = 0.019 \text{ min}^{-1}$ ,  $R^2 = 0.997$ ).

### 3.2. Phenol degradation kinetics in presence of Fe(II) as catalyst

Kinetic experiments were carried out with 1.05 mM phenol aqueous solutions in the presence of Fe(II) ions as catalyst. Fig. 2 shows kinetic curves in function of electrolysis time with catalyst's concentrations from 0.05 to 1.00 mM. It can be observed that phenol degradation rate increases with decreasing of Fe(II) concentration for concentrations larger than 0.1 mM. In these conditions, higher Fe(II) concentrations increased parasite reactions, consuming hydroxyl radicals, particularly due to reaction (6). Fe(II) concentrations lower than 0.1 mM are insufficient to catalyze the electro-Fenton system effectively because a small quantity of Fe(II) ions limits the production of hydroxyl radicals generated by reaction (2). These results underline once again that under our experimental conditions a concentration of 0.1 mM ferrous iron constitutes the optimal value for an effective oxidation of phenol in aqueous medium. Under these conditions, the complete degradation of a highly concentrated phenol solution (1.05 mM) takes place in less than 100 min even when the applied current is relatively weak. Fig. 2 shows also that the decrease in phenol concentration in function of electrolysis time is exponential, indicating a pseudo-first-order kinetic behavior. The graph of  $\text{Ln}([\text{Ph}]_0/[\text{Ph}]_t)$  in function of time at optimum conditions ( $[\text{Fe}^{2+}] = 0.1 \text{ mM}$ ) allows to found an apparent rate constant ( $k_{\text{app}}$ ) equal to  $0.037 \pm 0.003 \text{ min}^{-1}$  ( $R^2 = 0.999$ ).

The absolute rate constant of the reaction between phenol and hydroxyl radical was measured by competitive kinetics method [37,41] using 4-HBA as reference compound ( $k_{\text{abs}}(4\text{-HBA}) = 1.63 \times 10^9 \text{ M}^{-1} \text{ s}^{-1}$ ) [48]. Three experiments about the competitive degradation of 0.5 mM phenol and 0.5 mM 4-HBA for 30 min (Fig. 3) allowed to find the absolute rate constant of phenol degradation by hydroxyl radicals ( $k_{\text{abs}}(\text{Ph}/\bullet\text{OH})$ ), equal to  $(2.62 \pm 0.23) \times 10^9 \text{ M}^{-1} \text{ s}^{-1}$ . This value is in agreement



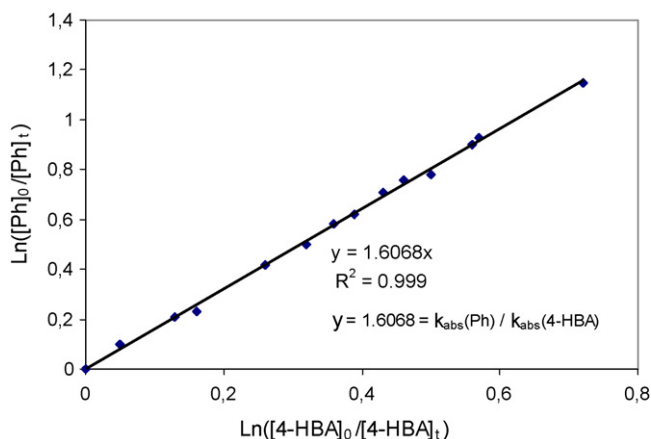


Fig. 3. Determination of the absolute rate constant of phenol degradation by hydroxyl radicals using competitive kinetics method [37,41]. Experimental conditions:  $V_0 = 125$  mL,  $I = 60$  mA and  $[Ph]_0 = [4-HBA]_0 = 0.5$  mM.

with  $k_{abs}$  values for hydroxylation reactions of aromatic compounds with hydroxyl radicals [48]. We have not found literature data for  $k_{abs}(Ph)$  at pH 3 for comparison. The  $k_{abs}(Ph)$  values reported in the literature are determined for pH 7.0 by pulse radiolysis method:  $6.6 \times 10^9 \text{ M}^{-1} \text{ s}^{-1}$  (pH 7 [49]) and  $1.4 \times 10^{10} \text{ M}^{-1} \text{ s}^{-1}$  (pH 7.6 [50]).

### 3.3. Mineralization of phenol aqueous solutions

Mineralization (i.e. oxidation to  $\text{CO}_2$  and water) experiments of 1.0 mM phenol aqueous solutions were conducted in optimum electrocatalytic conditions ( $[\text{Fe}^{2+}] = 0.1$  mM, pH 3) for different current density and volumes. Current was maintained constant ( $I = 300$  mA) and current density was changed by different surface areas of cathode. Mineralization of phenol in aqueous solution was monitored by measuring the TOC values evolution during electro-Fenton treatment. The decay of the TOC as a function of electrolysis time is shown in Fig. 4 which evidences the effect of the current density and the volume of treated solution on the mineralization efficiency. We could observe that, even with a constant applied current, it is

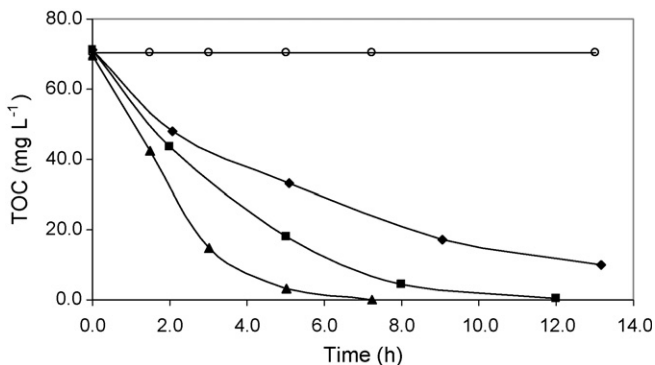
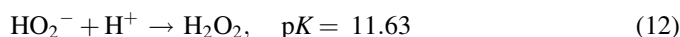
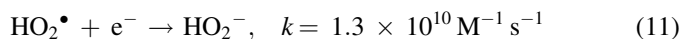
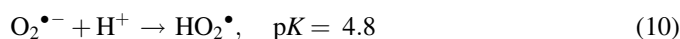
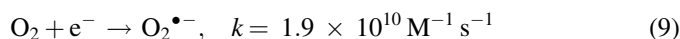


Fig. 4. Effect of current density ( $j$ ) and volume ( $V$ ) on the mineralization rate of phenol in aqueous media during electro-Fenton treatment. (◆)  $I = 300$  mA,  $j = 5.29 \text{ mA cm}^{-2}$ , and  $V_0 = 400$  mL; (■)  $I = 300$  mA,  $j = 5.29 \text{ mA cm}^{-2}$ , and  $V_0 = 150$  mL; (▲)  $I = 300$  mA,  $j = 2.56 \text{ mA cm}^{-2}$ , and  $V_0 = 150$  mL; (○) control experiment,  $I = 0$  mA,  $V_0 = 150$  mL, and carbon felt ( $6 \text{ cm} \times 17 \text{ cm}$ ). Experimental conditions:  $[\text{phenol}]_0 = 1.0$  mM,  $[\text{Fe}^{2+}] = 0.10$  mM and pH 3.

possible to increase mineralization efficiency, decreasing the current density and the volume. In fact, the electrochemical production of hydrogen peroxide, globally represented in Eq. (1), can be presented in four stages, limited by the first one [51,48].



So, the increase of the electrode (carbon felt) surface area approximately doubled the  $\text{O}_2$  quantity in contact with the cathode surface. Additionally, the initial volume reduction simply decreased phenol mass, increasing the TOC removal percentage. In best conditions, when a current efficiency of  $2.67 \text{ mA cm}^{-2}$  was applied, the total mineralization of 150 mL of 1 mM phenol solution was achieved at nearly 7 h. During control experiment, TOC loss due to phenol adsorption on carbon felt was negligible ( $<0.2\%$ ), confirming pseudo-first-order behavior observed in kinetic experiments.

### 3.4. Identification and evolution of aromatic intermediates of phenol oxidation

The identification of aromatic intermediates during phenol oxidation by hydroxyl radicals was performed by HPLC analyses by comparison of retention times ( $t_R$ ) with those of authentic products. These kinetics experiments were conducted at low current (60 mA) in order to favour the accumulation of hydroxylation reaction intermediates and thus facilitate kinetics study. Even under this low-current condition, the total removal of phenol and its aromatic by-products occurs in less than 150 min (Figs. 5 and 6).

The main initial reaction is the electrophilic addition of hydroxyl radical on the aromatic ring, leading to the formation of polyhydroxylated benzene derivatives (reactions (13) and (14)), such as hydroquinone, *p*-benzoquinone and catechol

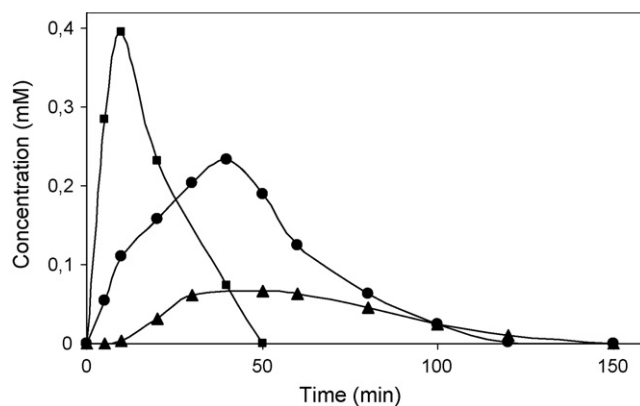


Fig. 5. Time-course of aromatic intermediates during the degradation of 1.05 mM phenol aqueous solution. (■) *p*-Benzoquinone; (●) catechol; (▲) hydroquinone. Experimental conditions:  $[\text{Fe}^{2+}] = 0.10$  mM,  $V_0 = 125$  mL, pH 3, and  $I = 60$  mA.

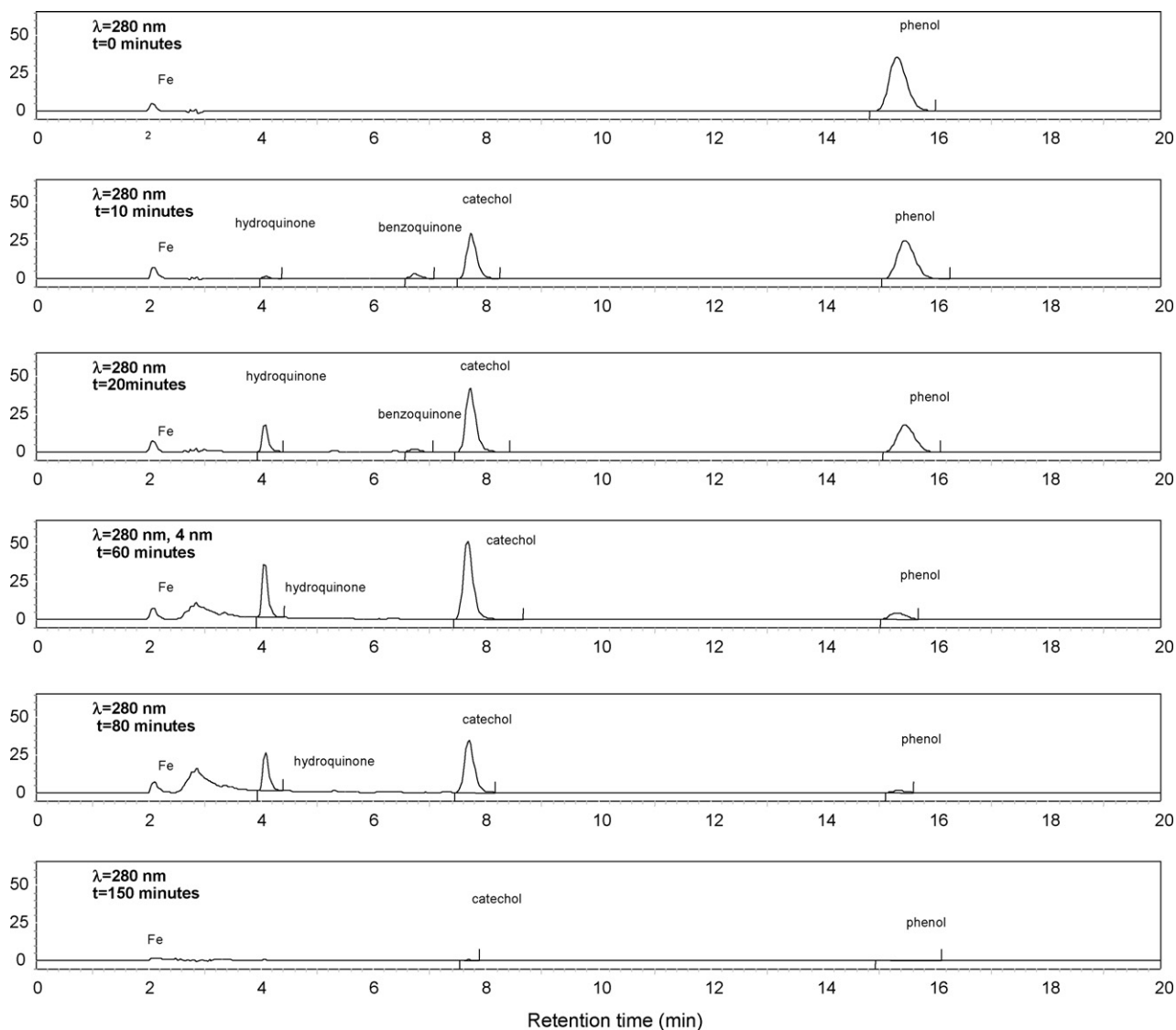
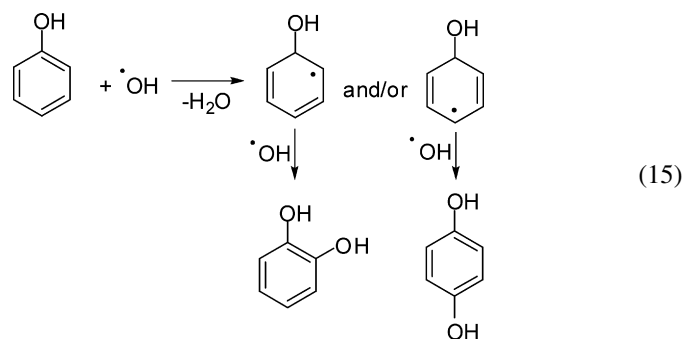
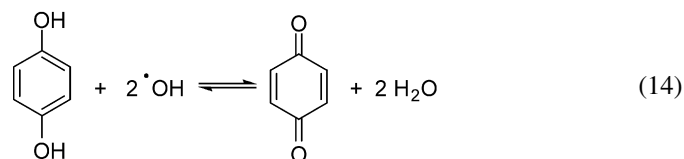
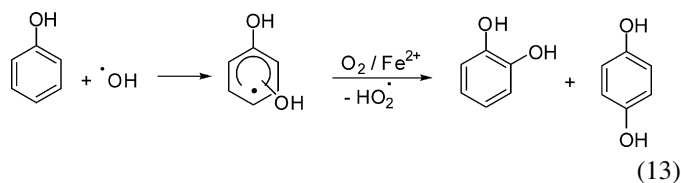


Fig. 6. Evolution of reverse-phase HPLC chromatograms (detection at 280 nm) during electro-Fenton treatment 1.05 mM phenol aqueous solution. Experimental conditions: pH 3,  $V_0 = 125$  mL, and  $[\text{Fe}] = 0.1$  mM. HPLC analysis conditions: Purospher RP-C18 column, eluent: water/methanol/acetic acid (79.2/19.8/1, v/v) and flow rate:  $0.8 \text{ mL min}^{-1}$ .

(Fig. 5). Hydroquinone, *p*-benzoquinone and catechol presented well-defined peaks at  $t_R$ : 4.2, 6.7, and 7.6 min (Fig. 6), respectively under our analysis conditions. These intermediates are in agreement with several studies conducted using other electrochemical-advanced oxidation techniques [16,29–33].

According to the *ortho* and *para* directing effect of the  $-\text{OH}$  group [52,53] during hydroxylation of aromatic compounds, catechol and hydroquinone appear as the major first aromatic by-products. Hydrogen atom abstraction reactions can occur simultaneously (reaction (15)), but only with smaller rate constants than those of electrophilic addition reactions [48].



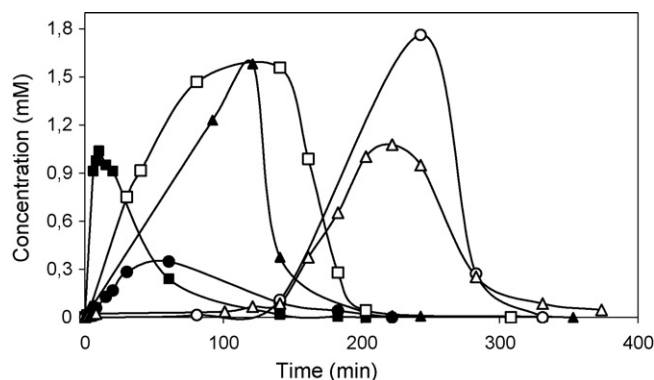


Fig. 7. Evolution of carboxylic acids formed during oxidation of phenol by electro-Fenton treatment: maleic (■), fumaric (●), succinic (▲), glyoxylic (□), formic (○), and oxalic (△) acids. Experimental conditions:  $[\text{phenol}]_0 = 2.50 \text{ mM}$ ,  $[\text{Fe}^{2+}] = 0.10 \text{ mM}$ ,  $[\text{Na}_2\text{SO}_4] = 50 \text{ mM}$ ,  $V_0 = 125 \text{ mL}$ , and  $I = 200 \text{ mA}$ .

As the medium is strongly oxidant, hydroquinone is quickly oxidized to 1,4-benzoquinone (reaction (14)). The small hydroquinone accumulation in the medium (Fig. 5) can be explained by its transformation to 1,4-benzoquinone and in parallel by its hydroxylation or mineralization reactions. In fact, absolute rate constants of 1,4-benzoquinone ( $k_{1,4\text{-BQ}} = 1.2 \times 10^9 \text{ M}^{-1} \text{ s}^{-1}$ ) [54] and hydroquinone ( $k_{\text{HQ}} = 1.0 \times 10^{10} \text{ M}^{-1} \text{ s}^{-1}$ ) [55] degradation by hydroxyl radicals show that hydroquinone has a greater tendency to be destroyed by hydroxyl radicals in comparison to 1,4-benzoquinone.

### 3.5. Identification and evolution of carboxylic acids

Electro-Fenton treated solutions were analysed in order to identify and quantify the carboxylic acids formed by the ring-opening reactions of phenol oxidation products (polyphenols and/or quinones). Phenol initial concentration and applied current were increased to 2.5 mM and 200 mA, respectively to identify generated carboxylic acids and follow their evolution during treatment (Fig. 7). Maleic, glyoxylic succinic and fumaric acids (detected at 9.0, 11.4, 14.3, and 17.0 min, respectively of retention time in our analysis conditions) were the predominant carboxylic acids formed in the earlier stages of the treatment. Maleic acid reached its maximum concentration at 15 min, being subsequently quickly degraded. Glyoxylic and succinic acids started to be formed in the first minutes reaching maximum concentrations at 2 h. The curves show the disappearance of the glyoxylic and succinic acids, followed by appearance of formic ( $t_R = 16.0 \text{ min}$ ) and oxalic ( $t_R = 7.5 \text{ min}$ ) acids as end products before total mineralization. The transformation of glyoxylic acid into oxalic acid by electrochemical-advanced oxidation methods was already reported by Boye et al. [22]. Traces of malonic, pyruvic and acetic acids (detected at  $t_R = 11.9$ , 10.6, and 17.4 min, respectively) were also detected.

In order to clarify the degradation mechanism, additional oxidation experiments with the most important aromatic intermediates were carried out at the same experimental conditions during 1 h (Figs. 8–10). Figs. 8–10 show the time-course of detected intermediates formed during oxidation of

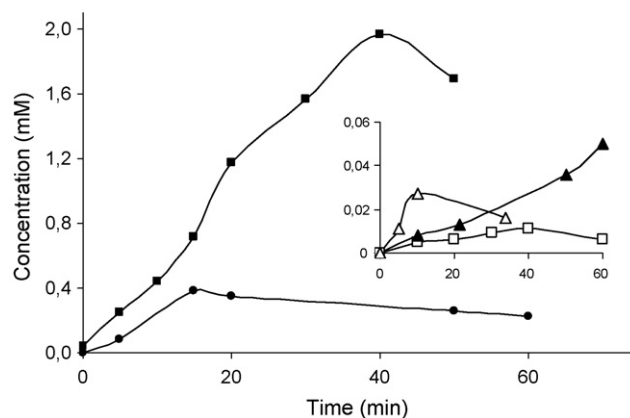


Fig. 8. Evolution of glyoxylic (■), fumaric (●), pyruvic (▲), malonic (△), and oxalic (□) acids during hydroquinone ( $C_0 = 2.50 \text{ mM}$ ) degradation under experimental conditions of Fig. 7.

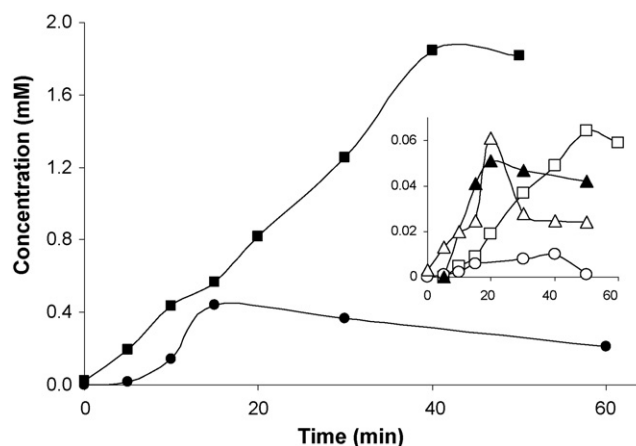


Fig. 9. Evolution of glyoxylic (■), fumaric (●), pyruvic (△), malonic (▲), oxalic (□), and maleic (○) acids during benzoquinone ( $C_0 = 2.50 \text{ mM}$ ) degradation under experimental conditions of Fig. 7.

aromatics by hydroxyl radicals. Dihydroxylated derivatives formed in the first reaction step were oxidized, leading to the formation of polyhydroxylated derivatives and/or quinones. Then, oxidative ring-opening reactions lead to formation of carboxylic acids. On the other hand, Fig. 4 highlights that

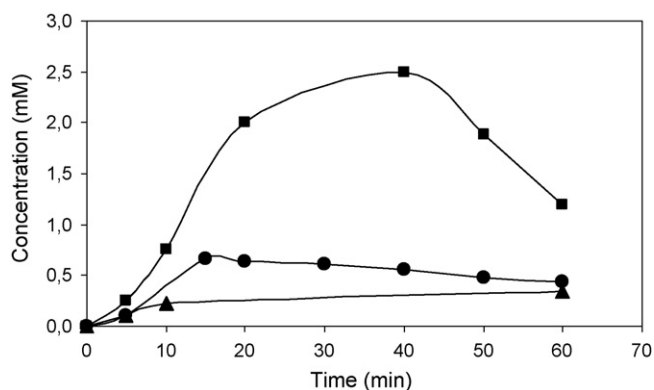


Fig. 10. Evolution of glyoxylic (■), fumaric (●), and succinic (▲) acids during electro-Fenton oxidation of catechol ( $C_0 = 2.50 \text{ mM}$ ) under experimental conditions of Fig. 7.

Table 2  
Carboxylic acids formed in earlier stages of carboxylic acids precursors degradation

Carboxylic acid precursor	Predominant products identified
Maleic	Glyoxylic, acetic, oxalic, formic
Fumaric	Glyoxylic, oxalic, formic
Succinic	Malonic, oxalic
Malonic	Oxalic
Pyruvic	Acetic, oxalic
Glyoxylic	Oxalic, formic
Acetic	Oxalic, formic
Oxalic	None
Formic	None

phenol mineralization in aqueous solution is effective from the beginning of the electro-Fenton treatment. Polyhydroxylated derivatives are unstable, which hinders their identification. So, in order to simplify the mechanism, we proposed complete reactions presenting ring-opening reactions directly from dihydroxylated derivatives.

During hydroquinone (Fig. 8) and 1,4-benzoquinone (Fig. 9) oxidation with hydroxyl radicals, glyoxylic and fumaric acids were predominantly formed. Traces of malonic, pyruvic, oxalic (Figs. 8 and 9) and maleic (Fig. 9) acids were also detected. It can be verified that the same carboxylic acids were essentially formed, confirming the redox equilibrium between 1,4-benzoquinone and hydroquinone (reaction (10)). Only in these experiments, pyruvic acid could be detected in the earlier minutes. Then, it was proposed that glyoxylic, fumaric and pyruvic acids were directly formed from hydroquinone/benzoquinone destruction. During catechol oxidation (Fig. 10), glyoxylic, fumaric and succinic acids were predominantly formed.

High concentrations of maleic or succinic acids were not observed during the degradation experiments of the main intermediates. However, both were predominantly formed during the first minutes of phenol degradation (Fig. 7). So, they were formed either by direct phenol destruction, or by unstable and/or not identified intermediates. For example, maleic acid

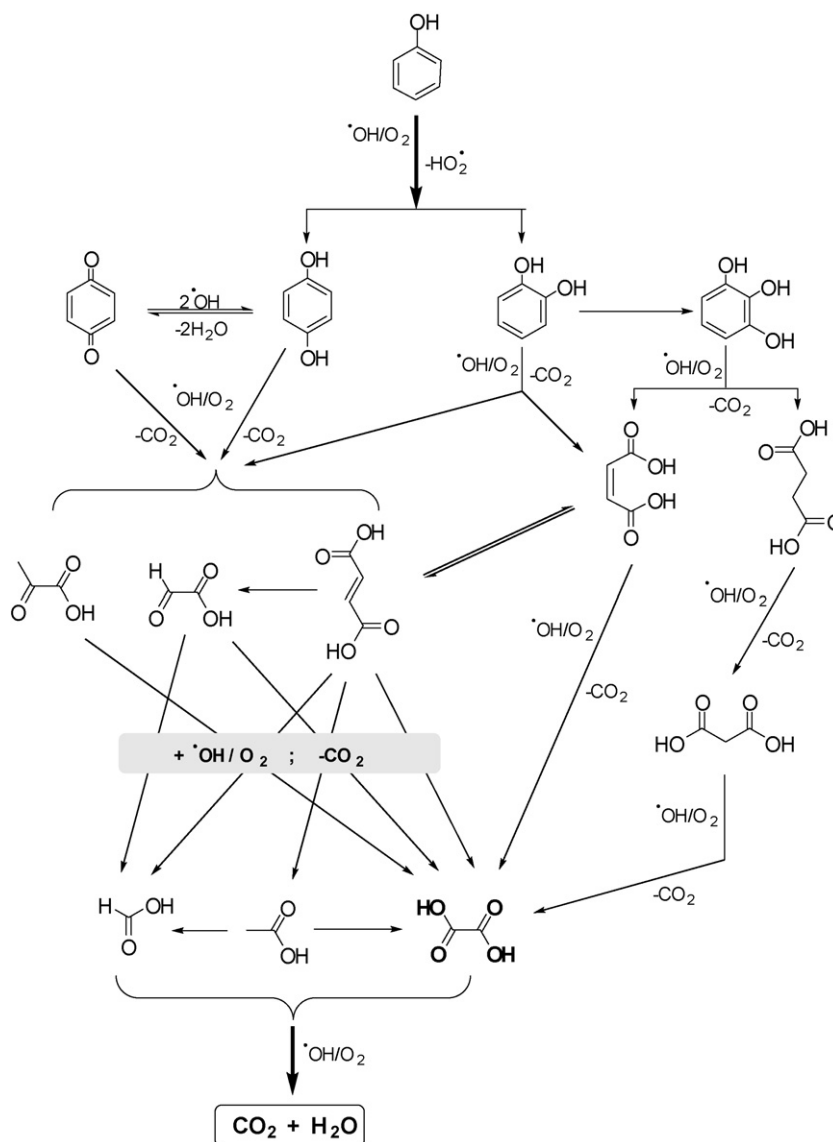
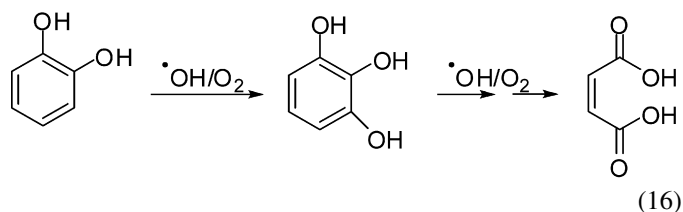


Fig. 11. General reaction sequence proposed for the mineralization of phenol in aqueous acid medium by hydroxyl radicals generated by electro-Fenton process.



can be formed from hydroxylated catechol (1,2,3-trihydroxybenzene) according to reaction (16):



### 3.6. Degradation pathway of phenol mineralization

In order to propose a complete degradation pathway of phenol in aqueous media by hydroxyl radicals, carboxylic acids were also degraded by electro-Fenton for 1 h. These experiments allowed to detect the first carboxylic acids produced during the reaction time of each acid (Table 2).

Considering the hydroxyl radical reaction kinetics, identification and evolution of aromatic and aliphatic reaction intermediates (Figs. 5–10 and Table 2), the molecular structures of carboxylic acids and the TOC measurements, an oxidative reaction pathway for phenol mineralization by hydroxyl radicals was proposed (Fig. 11).

## 4. Conclusions

In optimum experimental conditions, electro-Fenton process allowed to obtain total mineralization of phenol. Ferrous iron ions were the most effective catalysts with optimum concentration of 0.1 mM. Fixing constant currents and pH value about 3, smaller volumes and greater cathode surfaces allowed faster degradation. These results present tips to design, to compare and to optimize electrochemical reactors. It is important to remind that these optimum catalytic conditions were obtained considering phenol degradation. During electro-Fenton degradation of some other compounds, using iron as catalyst may lead to formation of complexes, changing iron concentration in the media. In these cases, other metal cations may present better results as catalyst.

Phenol oxidation by hydroxyl radicals follows a pseudo-first-order kinetics with an apparent rate constant of  $0.037 \text{ min}^{-1}$  under our experimental conditions (pH 3,  $V_0 = 125 \text{ mL}$ ,  $I = 60 \text{ mA}$ ,  $[\text{phenol}]_0 = 1.05 \text{ mM}$ ,  $[\text{Fe}^{2+}] = 0.1 \text{ mM}$ ). Using competition kinetics method, the absolute rate constant between phenol and hydroxyl radicals (pH 3) found to be  $(2.62 \pm 0.23) \times 10^9 \text{ M}^{-1} \text{ s}^{-1}$ . Hydroxylation of phenol generated benzoquinone, catechol and hydroquinone as the most important intermediates. Maleic, fumaric, succinic and glyoxylic were predominantly formed in the beginning, while oxalic and formic were the final products. These intermediates were also completely mineralized at the end of treatment. High-mineralization rates observed in first hours of treatment can be justified by higher reaction rate constant of hydroxyl radicals with aromatics in comparison with carboxylic acids and the formation of stables ferri-oxalate complexes. The total mineralization of phenol and its reaction intermediates evidences the efficiency of

the electro-Fenton as an advanced oxidation process in treatment of organic micropollutants.

## References

- [1] F.J. Rivas, F.J. Beltrán, O. Gimeno, P. Alvarez, J. Hazard. Mater. B96 (2003) 259–276.
- [2] W. Gernjak, T. Krutzler, A. Glaser, S. Malato, J. Caceres, R. Bauer, A.R. Fernandez-Alba, Chemosphere 50 (2003) 71–78.
- [3] J. Arana, E. Tello Rendon, J.M. Dona Rodriguez, J.A. Herrera Melian, O. Gonzalez Diaz, J. Pérez Pena, Chemosphere 44 (2001) 1017–1023.
- [4] R.L. Tatken, R.J. Lewis (Ed.), Registry of Toxic Effects of Chemical Substances, 1981–2 Edition, vol. 1, Publication No. 83–107, National Institute for Occupational Safety and Health (NIOSH), Cincinnati, 1983.
- [5] R.H. Dreisbach, Handbook of Poisoning: Prevention, Diagnosis and Treatment, Lang Medical Publications, Los Altos, CA, 1983pp. 401–405.
- [6] J.J. Pignatello, E. Oliveros, A. MacKay, Crit. Rev. Environ. Sci. Technol. 36 (2006) 1–84.
- [7] E.B. Azevedo, F.R.A. Neto, M. Dezotti, Appl. Catal. B: Environ. 54 (2004) 165–173.
- [8] D.H. Bremmer, A.E. Burgess, D. Houllemare, K.C. Namkung, Appl. Catal. B: Environ. 63 (2006) 15–19.
- [9] H. Utsumi, S.K. Han, K. Ichikawa, Water Sci. Technol. 38 (1998) 147–154.
- [10] E. Lypczynska-Kochany, Environ. Pollut. 61 (1993) 147–152.
- [11] R. Maciel, G.L. Sant-Anna Jr., M. Dezotti, Chemosphere 57 (2004) 711–719.
- [12] W. Wang, P. Serp Kalck, J.L. Faria, J. Mol. Catal. A: Chem. 235 (2005) 194–199.
- [13] J.M. Herrmann, Catal. Today 53 (1) (1999) 115–129.
- [14] S. Esplugas, J. Giménez, S. Contreras, E. Pascual, M. Rodríguez, Water Res. 36 (2002) 1034–1042.
- [15] S.G. Pouloupoulos, F. Arvanitakis, C.J. Philippopoulos, J. Hazard. Mater. B129 (2006) 64–68.
- [16] N. Belhadj Tahar, A. Savall, J. Electrochem. Soc. 145 (1998) 3427–3434.
- [17] I. Sirés, P.L. Cabot, F. Centellas, J.A. Garrido, R.M. Rodríguez, C. Arias, E. Brillas, Electrochim. Acta 52 (2006) 75–85.
- [18] E. Brillas, I. Sirés, C. Arias, P.L. Cabot, F. Centellas, R.M. Rodríguez, J.A. Garrido, Chemosphere 58 (2005) 399–406.
- [19] M.A. Oturan, J. Pinson, J. Phys. Chem. 99 (1995) 13948–13954.
- [20] M.A. Oturan, J. Appl. Electrochem. 30 (2000) 475–482.
- [21] M.A. Oturan, N. Oturan, C. Lahitte, S. Trevin, J. Electroanal. Chem. 507 (2001) 96–102.
- [22] B. Boye, M.M. Dieng, E. Brillas, Environ. Sci. Technol. 36 (2002) 3030–3035.
- [23] I. Sirés, F. Centellas, J.A. Garrido, R.M. Rodríguez, C. Arias, P.L. Cabot, E. Brillas, Appl. Catal. B: Environ. 72 (2007) 373–381.
- [24] I. Sirés, J.A. Garrido, R.M. Rodríguez, E. Brillas, N. Oturan, M.A. Oturan, Appl. Catal. B: Environ. 72 (2007) 382–394.
- [25] I. Sirés, N. Oturan, M.A. Oturan, R.M. Rodríguez, J.A. Garrido, E. Brillas, Electrochim. Acta 52 (2007) 5493–5503.
- [26] C. Flox, P.L. Cabot, F. Centellas, J.A. Garrido, R.M. Rodríguez, C. Arias, E. Brillas, Appl. Catal. B: Environ. 75 (2007) 17–28.
- [27] E. Brillas, B. Boye, M.M. Dieng, J. Electrochem. Soc. 150 (2003) E148–E154.
- [28] C. Flox, S. Ammar, C. Arias, E. Brillas, A.V. Vargas-Zavala, R. Abdelhedi, Appl. Catal. B: Environ. 67 (2006) 93–104.
- [29] C. Comninellis, C. Pulgarin, J. Appl. Electrochem. 21 (1991) 703–708.
- [30] N. Belhadj Tahar, A. Savall, J. Appl. Electrochem. 29 (1998) 277–283.
- [31] X. Li, Y. Cui, Y. Feng, Z. Xie, J. Gu, Water. Res. 39 (2005) 1972–1981.
- [32] J. Iniesta, P.A. Michaud, M. Panizza, G. Cerisola, A. Aldaz, C. Comninellis, Electrochim. Acta 46 (2001) 3573–3578.
- [33] E. Brillas, I. Sirés, C. Arias, P.L. Cabot, F. Centellas, R.M. Rodríguez, J.A. Garrido, Chemosphere 58 (2005) 399–406.
- [34] E. Fockede, A. Van Lierde, Water Res. 36 (2002) 4169–4175.

- [35] M.A. Oturan, J. Peiroten, P. Chartrin, A.J. Acher, *Environ. Sci. Technol.* 34 (2000) 3474–3479.
- [36] B. Gözmen, M.A. Oturan, N. Oturan, O. Erbatur, *Environ. Sci. Technol.* 37 (2003) 3716–3723.
- [37] M. Diagne, N. Oturan, M.A. Oturan, *Chemosphere* 66 (2007) 841–848.
- [38] M.A. Oturan, E. Brillas, *Port. Electrochim. Acta* 25 (2007) 1–18.
- [39] H. Türk, Y. çimen, *J. Mol. Catal. A: Chem.* 234 (2005) 19–24.
- [40] K.A. Barret, M.B. McBride, *Environ. Sci. Technol.* 39 (2005) 9223–9228.
- [41] K. Hanna, S. Chiron, M.A. Oturan, *Water Res.* 39 (2005) 2763–2773.
- [42] H. Christensen, K. Sehested, *Radiat. Phys. Chem.* 18 (1981) 723–731.
- [43] E. Neyens, J. Baeyens, *J. Hazard. Mater.* B98 (2003) 33–50.
- [44] J. Tonneau, in: *Tables de Chimie*, De Boeck Université, Bruxelles, 1991, pp. 45–49.
- [45] M.S. Wu, P.C.J. Chiang, *Electrochem. Commun.* 8 (2006) 383–388.
- [46] M. Ghaemi, L. Binder, *J. Power Sources* 111 (2002) 248–254.
- [47] J.C.A. Marr, J.A. Hansen, J.S. Meyer, D. Cacela, T. Podrabsky, J. Lipton, H.L. Bergman, *Aquat. Toxicol.* 43 (1998) 225–238.
- [48] G.V. Buxton, C.L. Greenstock, W.P. Helman, A.B. Ross, *J. Phys. Chem. Ref. Data* 17 (1988) 513–886.
- [49] R.J. Field, N.V. Raghavan, J.G. Brummer, *J. Phys. Chem.* 86 (1982) 2443–2449.
- [50] E.J. Land, M. Ebert, *Trans. Faraday Soc.* 63 (1967) 1181–1190.
- [51] F. Miomandre, S. Sadki, P. Audebert, R. Méallet-Renault, *Électrochimie—Des Concepts aux Applications*, Dunot, Paris, 2005, p. 82.
- [52] X. Fang, H.P. Schuchmann, C.V. Sonntag, *J. Chem. Soc. Perkin Trans. 2* (2000) 1391–1398.
- [53] X. Chen, R.H. Schuler, *J. Phys. Chem.* 97 (1993) 421–425.
- [54] G.E. Adams, B.D. Michael, *Trans. Faraday Soc.* 63 (1967) 1171–1180.
- [55] E. Heckel, A. Henglein, G. Beck, *Ber. Bunsen. Phys. Chem.* 70 (1966) 149–154.